Open access • Journal Article • DOI:10.1103/PHYSREVB.41.1934

Complex magnetic properties of the rare-earth copper oxides, R2CuO4, observed via measurements of the dc and ac magnetization, EPR, microwave magnetoabsorption, and specific heat — Source link

S. B. Oseroff, D. Rao, F. Wright, D. C. Vier ...+6 more authors

Institutions: San Diego State University, University of California, San Diego, Los Alamos National Laboratory

Published on: 01 Feb 1990 - Physical Review B (American Physical Society)

Topics: Absorption (logic), Order (ring theory), Magnetization, Magnetic anisotropy and Magnetic susceptibility

Title
Complex magnetic properties of the rare-earth copper oxides, R2CuO4, observed via measurements of the dc and ac magnetization, EPR, microwave magnetoabsorption, and specific heat.

Journal
Physical review. B, Condensed matter, 41(4)

ISSN
0163-1829

Authors
Oseroff, SB
Rao, D
Wright, F
et al.

Publication Date
1990-02-01

DOI
10.1103/physrevb.41.1934

Complex magnetic properties of the rare-earth copper oxides, R_2CuO_4, observed via measurements of the dc and ac magnetization, EPR, microwave magnetoabsorption, and specific heat

S. B. Oseroff, D. Rao, and F. Wright
San Diego State University, San Diego, California 92182

D. C. Vier and S. Schultz
University of California–San Diego, La Jolla, California 92093

J. D. Thompson, Z. Fisk, S-W. Cheong, and M. F. Hundley
Los Alamos National Laboratory, Los Alamos, New Mexico 87545

M. Tovar
Centro Atomico Bariloche 8400 Bariloche, Rio Negro, Argentina
(Received 7 August 1989)

We report the results of an extensive investigation of the magnetic properties of a large series of undoped R_2CuO_4 single crystals with $R \equiv$Pr, Nd, Sm, Eu, and Gd (which are the host compounds for the newly discovered series of electron cuprate superconductors) and mixture versions of the form $A_{2-x}B_xCuO_4$, with $A \equiv$Pr, Nd, Sm, Eu, or Gd, and $B \equiv$Gd, Tb, or Dy. We have measured dc and ac magnetization, microwave magnetoabsorption, EPR, and specific heat. These measurements reveal two characteristic transition temperatures associated with a novel complex magnetic behavior, including weak ferromagnetism, two sharp peaks in the low-field dc magnetization, an unusual anisotropy in the EPR resonance field for $R =$Gd, and two additional anisotropic microwave absorption modes. The higher characteristic transition temeperature at ~ 270 K is associated with antiferromagnetic ordering of the Cu moments which are strongly coupled within the CuO_2 layers. The lower, at ≤ 20 K, cannot be attributed to antiferromagnetic ordering of the R moments and is tentatively attributed to a spontaneous canted spin reorientation. An understanding of this magnetic behavior is important in order to ascertain its relationship to possible mechanisms of high-temperature superconductivity.

I. INTRODUCTION

The magnetic properties of the copper oxide high-transition-temperature (high-T_c) superconductors have been studied in great detail,[1] and there have been many theoretical suggestions that the magnetic properties of these materials play an important role in the underlying superconducting mechanism.[2] Most of this focus has been on the original La_2CuO_4, $YBa_2Cu_3O_{7-x}$, and related substitutional compounds, where antiferromagnetic order of the copper ions in the nonsuperconducting versions has been reported.[3] Fluctuating two-dimensional antiferromagnetic spin correlations in the CuO_2 planes has been reported to exist up to very high temperatures in these compounds, which persist even in samples that are doped to become superconductors, and the Néel temperature is reduced to zero.[4]

Until recently, all the different versions of cuprates studied were hole doped. Holes were added to the CuO_2 planes by replacing some La^{3+} by a divalent alkaline earth, or adding superstoichiometric amounts of oxygen.[5,6] Recently a new series of cuprate superconductors has been discovered of the form $R_{2-x}Ce_xCuO_4$ ($R =$Pr, Nd, Sm, or Eu)[7–9] and also with the Ce replaced by Th.[9,10] These materials are particularly interesting because electrons, rather than holes, in the CuO_2 planes are suggested to be the charge carriers involved in the high-T_c superconductivity.[11] The R_2CuO_4 with $R =$Pr through Gd form in a tetragonal crystal structure, with CuO_2 planes on which oxygen atoms are square-planar coordinated about copper, with no apical (out-of-plane) oxygen, rather than the quasioctahedrally arrangement observed for the K_2NiF_4-type structure.[12] The rare earths are coordinated by eight oxygens compared with nine oxygens in the case of La in La_2CuO_4. The space group of the R_2CuO_4 is an $I/4mmm$.[12]

We report the results of an extensive investigation of a large series of undoped R_2CuO_4 single crystals (with $R =$Pr, Nd, Sm, Eu, and Gd), and also mixture versions of $A_{2-x}B_xCuO_4$, with $A =$Pr, Nd, Sm, Eu, or Gd and $B =$Gd, Tb, or Dy. We have investigated the magnetic properties via five instrumental signals: dc magnetization, ac magnetization, EPR, microwave magnetoabsorption, and specific heat. Preliminary data on these systems have been reported previously.[13] We have identified eight specific features, henceforth called signatures, S-1, . . . , S-8, and two characteristic temperatures, T_h and T_L (defined in Sec. III A), which are indicated by rapid

changes or peaks in the instrumental signals corresponding to the specific property under investigation. An important conclusion of this work is a correlation between signatures measured by different techniques. Not all the signatures are found in every compound, although each of them is found in enough different compounds to be regarded as potentially present in the entire class.

The bulk of the experimental work reported here is a study of these signatures as a function of temperature, magnetic field amplitude and angle, rare-earth concentration, microwave frequency, etc., and therefore the totality constitutes a large body of data. The data are summarized in Sec. III, where we present the features observed in (III A) dc magnetization (signatures *S*-1, *S*-2, and *S*-3), (III B) ac susceptibility (features similar to dc magnetization), (III C) microwave magnetoabsorption (signatures *S*-4, *S*-5, and *S*-6), (III D) EPR of Gd^{3+} (signature *S*-7), and (III E) specific heat (signature *S*-8).

We regard the clarification of the unusual magnetic properties of these compounds to be important for furthering our understanding of copper-oxide superconductivity from two perspectives. The first is obvious; there may be a magnetic origin to the underlying superconducting mechanism. The second is that, even if there is no specific magnetic superconducting mechanism, once the complex magnetic properties of these compounds are understood, it will be possible to utilize these experimental signals and their associated signatures as powerful probes into the internal states of the system. An explanation of the absence, presence, or changes that may occur in these signatures as the systems are doped into becoming superconductors may provide discriminating tests of the alternate models that are proposed.

II. EXPERIMENTAL DETAILS

Thin, platelike crystals of R_2CuO_4 have been grown from PbO and CuO fluxes with the crystallographic *c* axis parallel to the thin dimension.[14] In the case of Gd_2CuO_4, refinement of the x-ray spectra gives lattice constants $a=b=3.892$ Å and $c=11.878$ Å with a site occupancy of 0.99(2) for Gd and 1.01(5) for oxygen, indicating that the crystals grow at, or very close to, the stoichiometric composition.[14] Samples grown with PbO flux, when examined by electron-microprobe analysis, show that the Pb content, if any, is less than 1 at. % of Cu. In contrast to La_2CuO_4, the electronic and magnetic properties of the R_2CuO_4 are insensitive to anneal in various gas atmospheres, suggesting that the oxygen content is highly stable.[14]

The microwave magnetoabsorption and EPR experiments were performed on 9 and 35 GHz spectrometers, operated in the conventional derivative absorption mode at temperatures between 1.7 and 600 K. The dc magnetization, M_{dc}, was measured with a SQUID magnetometer for temperatures between 1.8 and 400 K and fields up to 50 kOe, or with a vibrating sample magnetometer for temperatures between 77 and 700 K. Specific heat, C_p, was measured from 1.6 to ~30 K in a small-mass calorimeter described in detail elsewhere.[15] The ac susceptibility was measured between 4 and 300 K and from 1 to 1000 Hz in a system described elsewhere.[16]

A. dc Magnetization

In Fig. 1 we present the inverse of the dc magnetic susceptibility (measured in a 10 kOe field applied parallel to

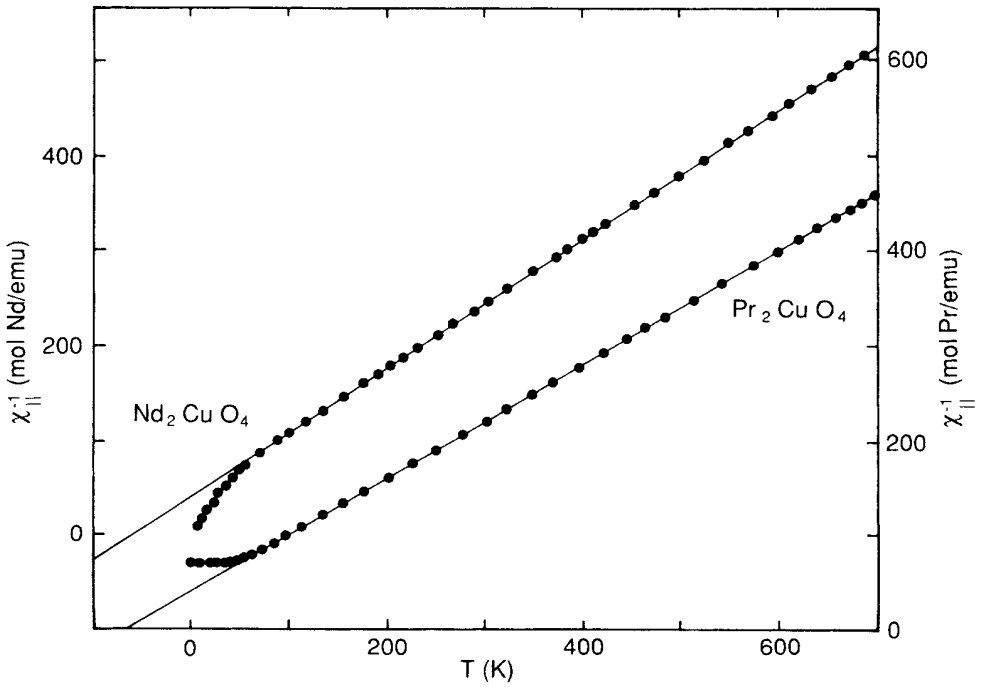

FIG. 1. Inverse magnetic susceptibility χ^{-1} of Pr_2CuO_4 and Nd_2CuO_4 as a function of temperature. Measurements were made with a 10 kOe field applied parallel to the CuO_2 planes. The solid lines represent the best fit to Curie-Weiss law with $\mu_{eff}(Pr)=3.65\pm0.05\mu_B$, $\theta_{Pr}\sim-65$ K, $\mu_{eff}(Nd)=3.56\pm0.05\mu_B$, and Nd ~-60 K.

the CuO_2 planes) as a function of temperature between 2 and 700 K, for both Pr_2CuO_4 and Nd_2CuO_4. We note that the curvature below ~70 K is understood as being due to the crystal-field splitting of the low-lying states. Above ~300 K the magnetization for all the systems studied (see Table I) is linear in applied magnetic field, with a magnetic moment per formula unit corresponding to that expected for the trivalent rare-earth ion. However, below ~300 K we find that, in contrast to the behavior shown in Fig. 1, other R compositions of these materials exhibit a nonlinearity[17] that becomes evident as the field is reduced, and evolves into a sharp peak when the field is in the vicinity of 1–10 Oe. Another peak may be found at temperatures ≤ 20 K. We identify these peaks as signatures S-1 and S-2 as follows.

1. S-1 and S-2: Sharp peaks in the temperature dependence of the low-field M_{dc}

In Fig. 2 we present the dc magnetization, M_{dc}, measured in a field of ~1 Oe (applied parallel to the CuO_2 planes), as a function of temperature for a $EuTbCuO_4$ sample. Two sharp peaks are observed. The higher-temperature peak, which we call signature S-1, always has an onset at 275±10 K. Values of the onset are presented in Table I for compounds exhibiting the signature S-1. We define its characteristic temperature, T_h, as the temperature at which M_{dc} peaks when measured in a field of 1 Oe. The lower-temperature peak we call signature S-2 and its characteristic temperature, T_L, is defined similarly to T_h. Other systems which also exhibit the two signature peaks S-1 and S-2 are indicated in Table I. The relative amplitude of the two peaks is dependent on the

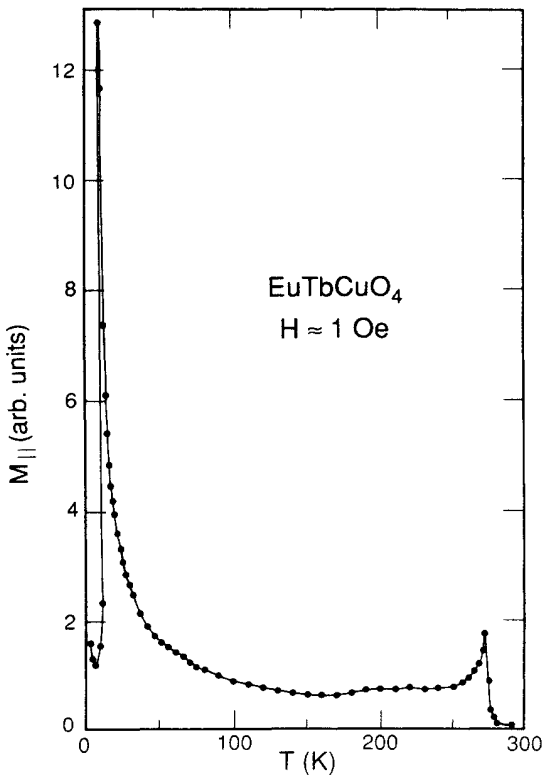

FIG. 2. The dc magnetization vs temperature for $EuTbCuO_4$ measured in a field of about 1 Oe applied parallel to the a-b plane. The two peaks at 270 and 10 K are associated with the high and low characteristic temperatures, T_h and T_L, respectively. These peaks depend on the field angle to the a-b plane as discussed in the text. The solid line is a guide to the eye.

TABLE I. Presence of signatures for R_2CuO_4 samples studied. S-1 to S-8 are measured signatures discussed in the text. An entry of Y (or N) in the table means that the signature was (or was not) observed for the sample indicated. An asterisk (*) means that the EPR of the R moment was not observed. A blank means the sample was not tested for that signature.

System \ Signature	S-1 (onset)	S-2 (T_L)	S-3	S-4	S-5	S-6 (peak)	S-7	S-8 (peak)
Pr_2CuO_4	N	N	N	N	N	N	*	N[a]
$PrGdCuO_4$	N	N	N	N	N	N	N	
Nd_2CuO_4	N	N	N	N	N	N	*	Y (~1.5 K)
$Nd_{1.8}Gd_{0.2}CuO_4$	N	N	N	N	N	N	N	
$NdTbCuO_4$	N	N	N	N	N	N	*	
Sm_2CuO_4	N	N	N	N	N	N	*	Y (5.95 K)
$SmGdCuO_4$	Y (268 K)	Y (11 K)	Y	Y	Y		Y	
Eu_2CuO_4	N	N	N	Y[c]			*	
$Eu_{1.97}Gd_{0.03}CuO_4$	Y	N (<2 K)	N	Y	Y	N	Y	
$Eu_{1.8}Gd_{0.2}CuO_4$	Y (265 K)	N (<2 K)	Y	Y	Y	N	Y	
$EuGdCuO_4$	Y (266 K)	Y (9 K)	Y	Y	Y	Y (10 K)	Y	
$Eu_{0.2}Gd_{1.8}CuO_4$	Y (270 K)	Y (18 K)	Y	Y	Y	Y (19 K)	Y	
$EuTbCuO_4$	Y (275 K)	Y (10 K)	Y	Y	Y	Y (10 K)	*	N[b]
$EuDyCuO_4$	Y (275 K)	Y (18 K)	Y					
Gd_2CuO_4	Y (268 K)	Y (19 K)	Y	Y	Y	Y (18 K)	Y	Y (6.5 K)
$GdTbCuO_4$	Y	Y (18 K)	Y	Y	Y	Y (18 K)	Y	

[a]Possible nuclear Schottky anomaly.
[b]Down to 1 K.
[c]Observed onset is ~210 K compared to ~280 K for all other "Y" S-4 entries.

rare earths used. However, T_h is basically independent of the particular rare-earth constituents used, with a value of 260±15 K. In contrast, T_L is a function of both the rare earths used and their relative concentration. Values of T_L are presented in Table I for compounds exhibiting the signature S-2. In most cases for which the S-1 peak is observed, the S-2 peak is also found, unless its temperature has been shifted below our limit of observation (2 K) by the choice of rare-earth relative concentrations.

Both of the peaks are broadened and move to lower temperature when the magnetic field is increased to only 10–100 Oe, and they are smeared sufficiently so as to be only weakly or not at all detected with respect to a large paramagnetic magnetization for fields above 1 kOe. There is evidence for a mild difference between field-cooled and zero-field-cooled data. At temperatures below the S-1 peak we find a large anisotropy with respect to the angle of the applied magnetic field to the CuO_2 planes, and when the field is applied parallel to the c axis there is no indication of either peak.[17]

2. S-3: *Weak ferromagnetism*

Whenever the S-1 peak is observed, we also find a nonlinear field dependence in the initial magnetization for $T < T_h$. This effect is illustrated in Fig. 3, where hysteresis loops for small magnetic fields (±100 Oe applied parallel to the CuO_2 planes) are presented for $EuTbCuO_4$ at several temperatures. At sufficiently high fields M_{dc} becomes linear, with the magnetic moment expected for the corresponding rare-earth ion, and when extrapolated back to zero defines an internal field, $H_i(\theta)$, where θ refers to the angle between the a-b plane and the applied magnetic field. This signature property is further illustrated in Fig. 4, where curves of M_{dc} versus field up to 6 kOe are presented for six systems that exhibit this feature, and one which does not (Pr_2CuO_4). From these data we obtain $H_i(0)=800\pm200$ Oe for all samples that exhibit the S-3 signature, whereas the value of the field after which the magnetization becomes linear is dependent on the particular rare earth used. As can be seen in Fig. 4, the value of this field varies from ≤ 100 Oe for $EuTbCuO_4$, Gd_2CuO_4, or $GdTbCuO_4$ to ~ 1000 Oe for $Eu_{1.8}Gd_{0.2}CuO_4$ or $SmGdCuO_4$.

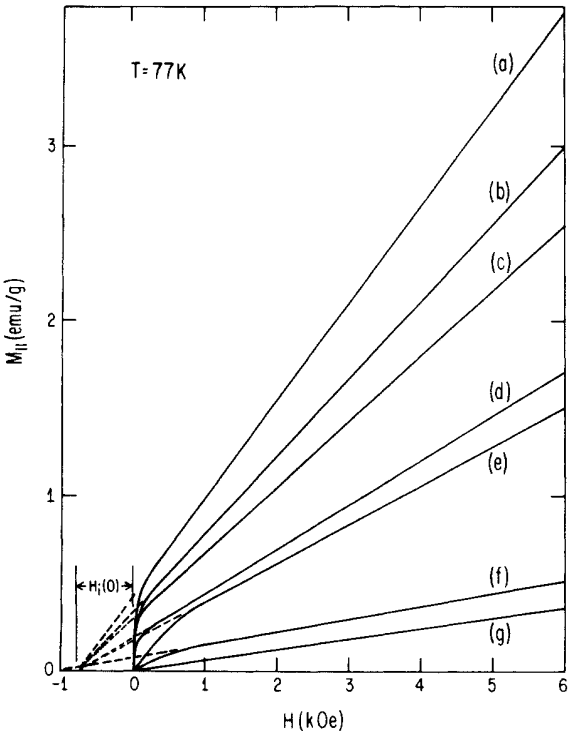

FIG. 4. The dc magnetization, M_{dc}, vs magnetic field applied parallel to the a-b plane for the following compounds at a temperature of 77 K: (a) $GdTbCuO_4$, (b) $EuTbCuO_4$, (c) Gd_2CuO_4, (d) $EuGdCuO_4$, (e) $SmGdCuO_4$, (f) $Eu_{1.8}Gd_{0.2}CuO_4$, and (g) Pr_2CuO_4. The linear dependence at higher fields corresponds to the paramagnetism of the R ions. When extrapolated back to zero M_{dc}, all the lines but the one for Pr_2CuO_4 intersect near a reverse field, $H_i(0)=800$ Oe.

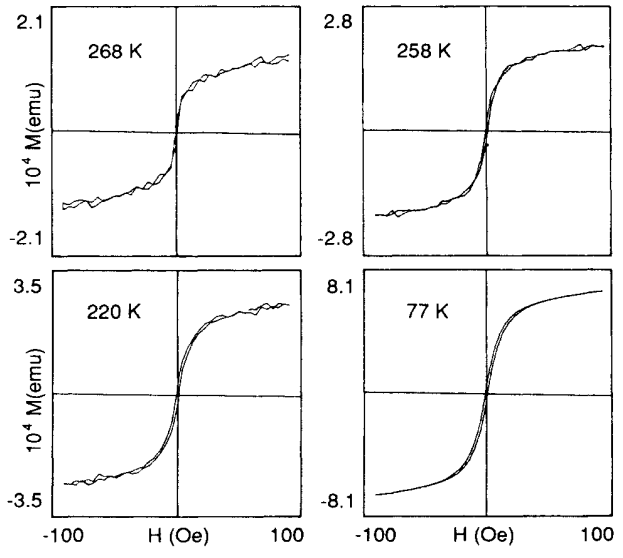

FIG. 3. Hysteresis loops for a 2 mg single crystal of $EuTbCuO_4$ with the field applied parallel to the CuO_2 planes for several temperatures. Notice that the true zero-field moment is negligible.

$H_i(\theta)$ is found to be independent of temperature from the onset at T_h down to T_L, and has a complex behavior at lower temperatures. These properties are illustrated in Fig. 5, where M_{dc} versus H curves similar to that in Fig. 4 are presented for a series of temperatures for $EuTbCuO_4$. From the data in Fig. 5(b) one sees that for $EuTbCuO_4$, T_L occurs at ~ 10 K, where a rapid change in the character of the initial magnetization sets in.

When M_{dc} is measured with the applied field making an angle θ to the a-b plane, the linear magnetization region is not established until higher values of field, which we find qualitatively to depend as $1/\cos\theta$. The extrapolated intercept, $H_i(\theta)$, is also a function of angle, and an example of such data are presented in Fig. 6 for Gd_2CuO_4 at 77 K. The solid line is a fit to the data of the form, $H_i(\theta)=H_i(0)\cos\theta$. Because we experimentally measure

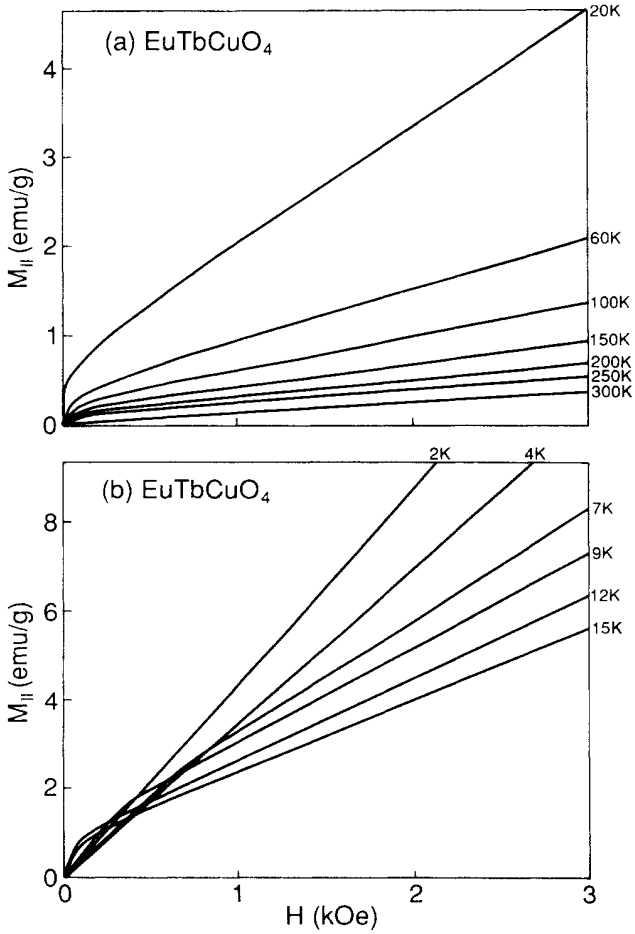

FIG. 5. Magnetization for a single crystal of $EuTbCuO_4$ as a function of magnetic field applied parallel to the CuO_2 planes for several temperatures. An extrapolation of the linear, high-field portion of each curve in (a) intersects at a common point, $M \sim 0.02$ emu/g and $H \sim -700$ Oe.

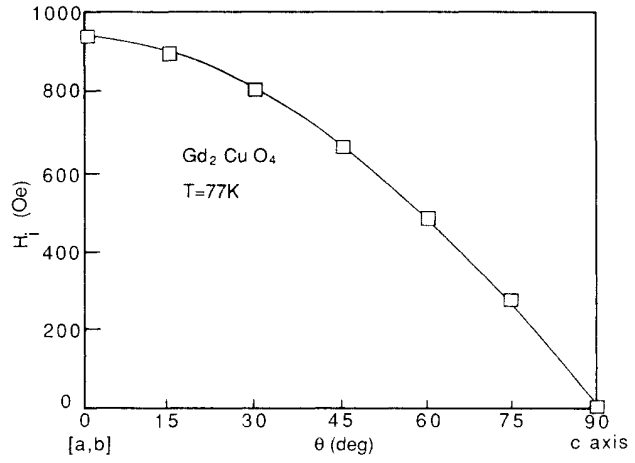

FIG. 6. The internal field H_i for Gd_2CuO_4 at 77 K, obtained by extrapolating to zero magnetization once the linear region in the magnetization has been established, is given as a function of angle of the applied field to the CuO_2 planes. The solid line corresponds to the best fit to $H_i(\theta)=H_i(0)\cos\theta$ with $H_i(0)=930$ Oe. The $\cos\theta$ dependence arises because we only measure the component of M_{dc} in the direction of the applied field, as discussed in the text.

the component of M_{dc} along the applied field direction, these results suggest that (1) only the component of the applied field in the *a-b* plane is important to fully "set" H_i, and (2) once "set," H_i always has its direction in the *a-b* plane, with a fixed value of ~ 800 Oe, independent of the angle θ of the applied field.

In Fig. 7 hysteresis loops are presented for Gd_2CuO_4 at 77 K, with the field applied at three different angles: (a): $\theta=0$, (b): $\theta=60°$; and (c): $\theta=90°$. From Figs. 3 and 7 it is seen that some finite hysteresis cannot be ruled out, but if there is a coercivity, it is less than a few Oe, and the remanence is less than a few percent of the extrapolated M_{dc} at $H=0$. In Fig. 8 we present M_{dc} as a function of θ for Gd_2CuO_4 in a 10 Oe field at 77 K. A similar anisotropic behavior has been found in all the systems where an enhanced initial magnetization is found.

Some of the systems, such as the series $Eu_{2-x}Gd_xCuO_4$ (for $0.2 \le x \le 2$), do not show appreciable anisotropy in the *a-b* plane ($< 15\%$). However, other systems, such as $EuTbCuO_4$, do exhibit a large anisotropy of M_{dc} (a factor of 2) as a function of orientation angle of the magnetic field in the *a-b* plane, although we still find the same extrapolated value for H_i within the experimental error.

B. ac susceptibility

We have measured the ac susceptibility, χ_{ac}, of several samples as a function of frequency (1–1000 Hz), field (0.1–10 Oe), and temperature (6–300 K). The dependence on applied field magnitude, angle of field, and rare-earth concentration is similar to that found by the dc magnetization measurements. When χ_{ac} is measured as a function of temperature in a fixed weak magnetic field (1 Oe) we also find two peaks, at T_h and T_L, independent of frequency for the range studied. Similar to

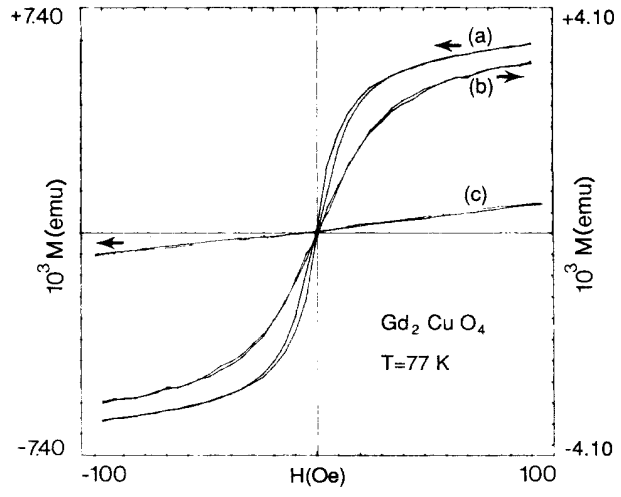

FIG. 7. Hysteresis loops of a 21 mg single crystal of Gd_2CuO_4 measured at 77 K with the field applied (a) parallel to the CuO_2 planes, (b) 60° from them, and (c) parallel to the *c* axis. The arrows indicate different scales used for the magnetization.

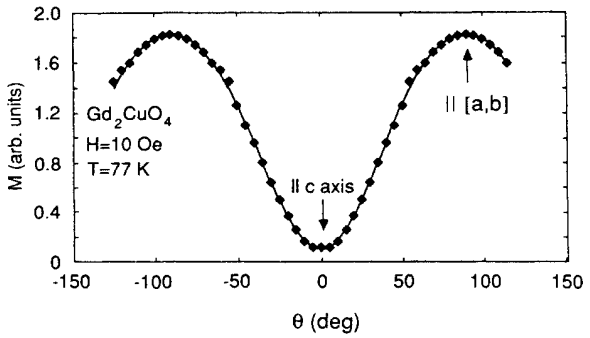

FIG. 8. The magnetization as a function of angle in a 10 Oe field at 77 K for Gd_2CuO_4. The solid line is the best fit to $M(\theta)=M_0+K_1\sin^2\theta+K_2\sin^4\theta$, with $M_0=0.10\pm0.01$, $K_1=2.37\pm0.08$, and $K_2=0.65\pm0.05$.

the dc magnetization, we found that both maxima get weaker, broader, and shift to lower temperatures when the applied magnetic field is increased. In Fig. 9 we present data for χ_{ac} as a function of temperature in the vicinity of T_h for $GdTbCuO_4$ measured at three different values of the magnetic field (applied parallel to the *a-b* plane).

C. Microwave magnetoabsorption signals

For samples which exhibit the *S*-1 to *S*-3 signatures but do not contain any Gd, a typical EPR spectrometer field sweep at 9 GHz for $T_L < T < T_h$ is shown in Fig. 10. In general, there are two signals. If the applied magnetic field is parallel to the CuO_2 planes, as in Fig. 10, one signal occurs at very low magnetic fields, and the other at

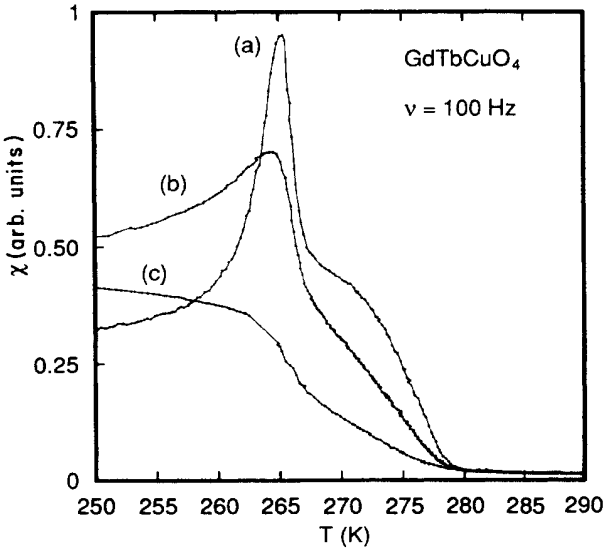

FIG. 9. ac susceptibility as a function of temperature for a ~15 mg single crystal of $GdTbCuO_4$ measured at a frequency of 100 Hz for different applied fields parallel to the planes: (a) 1 Oe, (b) 3 Oe, and (c) 10 Oe. No frequency dependence on the position of the peak has been observed.

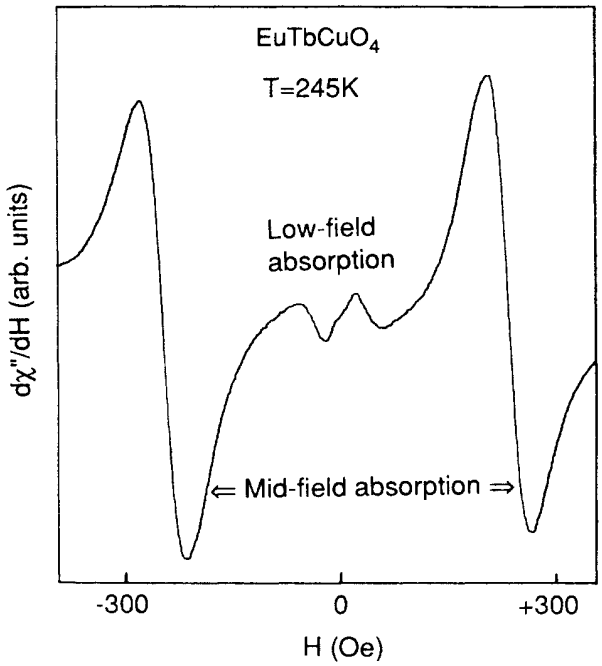

FIG. 10. Spectra for a 0.5 mg single crystal of $EuTbCuO_4$ measured at 245 K and 9.2 GHz with the field applied parallel to the CuO_2 planes. There are two signals that we call the low-field and midfield absorptions as discussed in the text.

intermediate values, when compared to $H_r \sim 3$ kOe for normal $g=2$ EPR signals. The signal occurring at intermediate magnetic field values we call the midfield absorption, signature *S*-4, and the signal ocurring at low magnetic fields we call the low-field absorption, signature *S*-5.

The *S*-4 and *S*-5 signals first appear at ~270 K, and their amplitude is largest at temperatures near T_h (as defined in Sec. III A). As the temperature is lowered below T_h, the amplitude steadily decreases, and the sig-

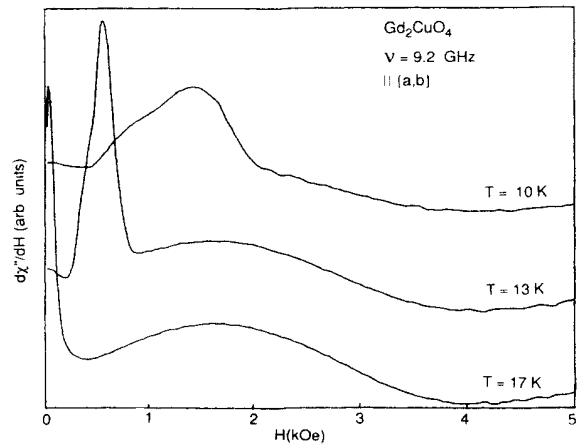

FIG. 11. Microwave magnetoabsorption at 9 GHz as a function of magnetic field applied parallel to the CuO_2 planes for Gd_2CuO_4 at different temperatures below T_L. The broad weak absorption is the EPR of Gd^{3+} and the sharper, stronger absorption is the signature *S*-6 as discussed in the text.

nals eventually disappear at temperatures near T_L. At T_L a new magnetoabsorption signal appears, which we call signature *S*-6. Its signal is shown in Fig. 11 for Gd_2CuO_4 at three temperatures below T_L (the broad, weak signal present is the EPR of Gd^{3+}). We now present the behavior of the microwave magnetoabsorption signals *S*-4, *S*-5, and *S*-6.

1. S-4: midfield absorption signal

In Fig. 12 we present the temperature dependence of the magnetic field at which the maximum value of the midfield absorption signal occurs, H_p (as identified in the inset of Fig. 13) for θ values of 0 and 85°, and for a frequency of 35 GHz. The line shape of the midfield absorption makes it difficult to define a center value, which is why we use H_p as defined in Fig. 13 for most of the data analysis. At all temperatures between T_L and T_h, the variation of H_p with θ is as shown in Fig. 13. The solid lines are a fit to the data of the form $H_p = K/\cos\theta$, where K depends on both the microwave frequency and the rare earths used. Fig. 14 illustrates the frequency dependence of *S*-4, where we find that K is typically a factor of 2–3 larger at 35 GHz than at 9 GHz.

The intensity of the midfield absorption signal as a function of temperature for $EuTbCuO_4$ is shown in Fig. 15. A maximum is observed at a temperature near T_h. The midfield absorption signal amplitude was found to be strongly dependent on (1) the frequency of the field modulation applied parallel to the dc magnetic field, (2) the angle of the dc magnetic field in the *a-b* plane (the rf magnetic field was also kept parallel to the *a-b* plane, but always perpendicular to the dc field), and (3) the angle of the rf magnetic field out of the plane. The midfield absorption amplitude does not go to zero as the dc and rf fields become parallel, as would be the case for a standard EPR signal. The intensity of the midfield absorption signal is very large by EPR standards. The integrated signal corresponds to a paramagnetic moment with an effective

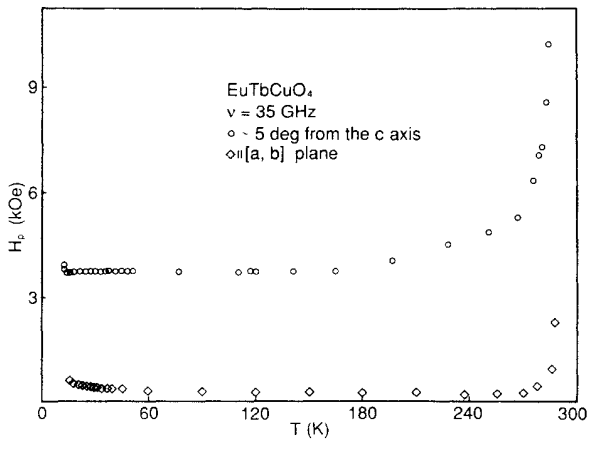

FIG. 12. The value of H_p at 35 GHz for $EuTbCuO_4$ (as identified in the Fig. 13 inset) as a function of temperature for the two field angles, θ, is indicated. The onset at high temperature correlates with T_h.

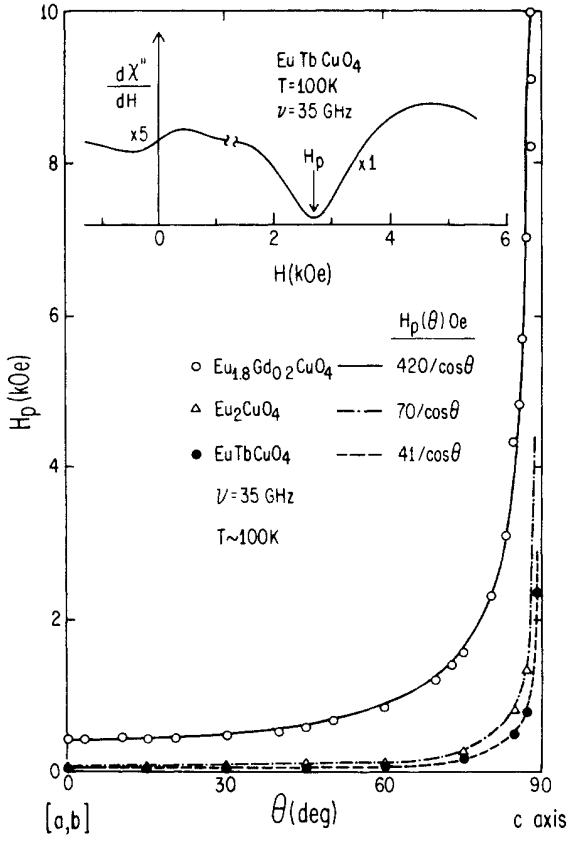

FIG. 13. The magnetic field position of the midfield absorption peak, H_p (as indicated in the inset), as a function of the magnetic field angle θ, for the samples indicated. The solid curves are a fit to the form $H_p(\theta) = H_p(0)/\cos\theta$. Inset: The 35 GHz EPR spectrometer output ($d\chi''/dH$) as a function of magnetic field for $EuTbCuO_4$ at 100 K.

number between 3 and 100 Bohr magnetons per formula unit, depending on the angle, temperature, and system.

In the inset of Fig. 15 we present the angular dependence of the peak-to-peak linewidth for $EuTbCuO_4$ at 245 K, which is found to exhibit a $1/\cos\theta$ dependence. Note that in this case the midfield absorption peak-to-peak linewidth and center position, H_r, are easily interpreted (see Fig. 10). H_r (not shown) is also found to vary as $1/\cos\theta$. For the $(Eu_{1-x}Gd_x)_2CuO_4$ system there is a correlation of the intensity with increasing Gd concentration.

2. S-5: low-field absorption signal

The low-field absorption appears to be related to the signature *S*-1. It also behaves in a similar manner to the midfield absorption, in that they both exhibit a $1/\cos\theta$ anisotropic behavior and both signals die out as T decreases to T_L. However, their relative intensity depends on the particular R_2CuO_4 system. The low-field absorption signal first appears 5–10 K below the appearance of the midfield absorption.

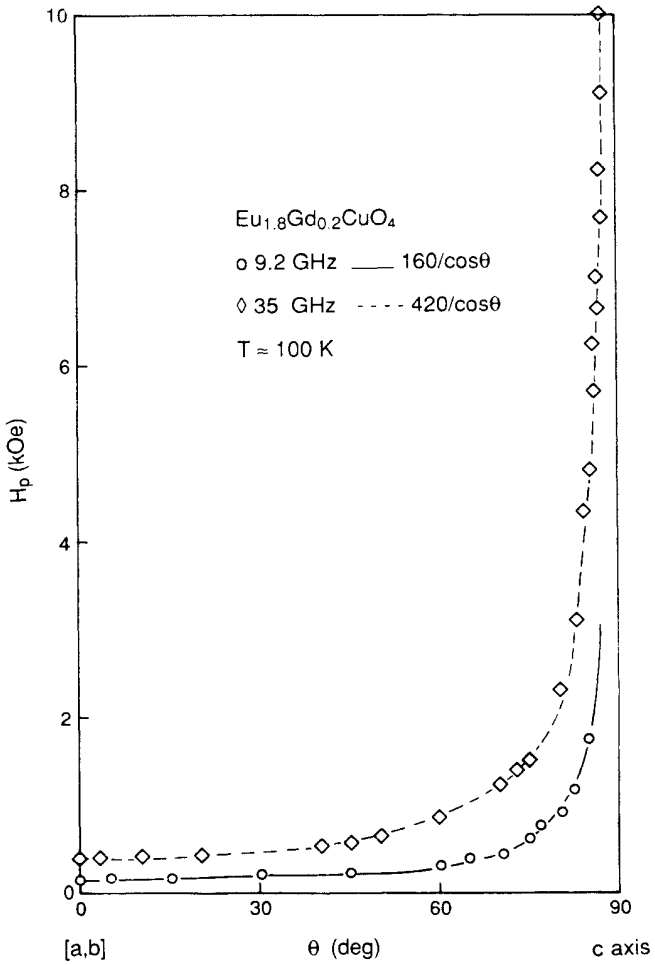

FIG. 14. The field at which the midfield absorption peaks, H_p, as a function of angle with the CuO_2 planes for $Eu_{1.8}Gd_{0.2}CuO_4$ measured at 100 K for frequencies of 9.2 and 35 GHz. The lines are the best fit to the data with $H_p(\theta)=H_p(0)/\cos\theta$.

3. *S-6: Magnetoabsorption signal observed at or below* T_L

In Fig. 11 we presented the *S*-6 signal for Gd_2CuO_4 at three different temperatures. Note that as the temperature is lowered, the signal peak is suppressed and moves to higher fields. If instead of sweeping field at a fixed temperature, one sweeps temperature at fixed magnetic field, the spectrometer output for signature *S*-6 is as shown in Fig. 16. A signal peak is observed that is suppressed and shifts to lower temperature as the field is increased. (This behavior is similar to that observed for signature *S*-2.) From a study of peak temperature as a function of dc field magnitude and angle, it is found that the temperature shift is only dependent on the component of field in the *a-b* plane. This property is illustrated in the inset of Fig. 16, where we present values of the *S*-6 peak temperature for fields up to 5 kOe applied parallel to the *a-b* plane (solid squares), and also for a constant field of 5 kOe applied at various θ (open squares), where the field value plotted is 5 kOe $\cos\theta$.

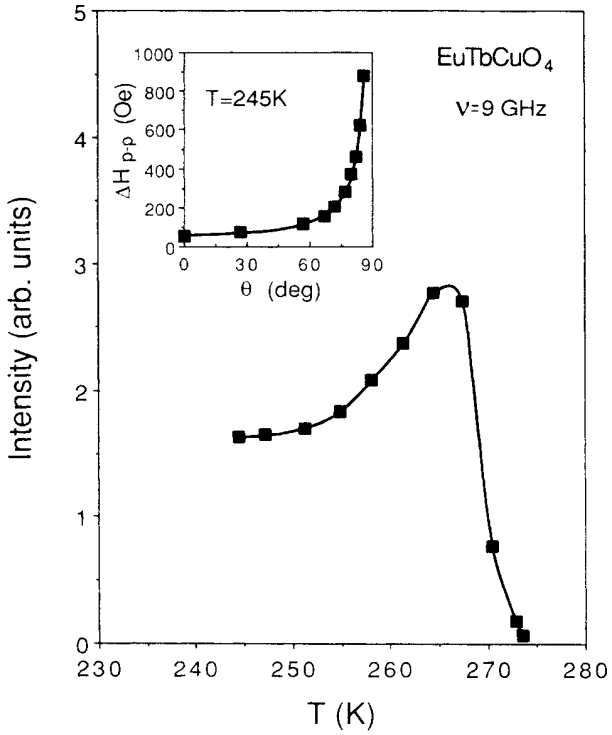

FIG. 15. Temperature dependence of the intensity (amplitude times linewidth squared) of the midfield absorption of $EuTbCuO_4$ measured at 9.2 GHz with the field applied parallel to the CuO_2 planes. Inset: The peak-to-peak linewidth measured at 245 K with the magnetic field making an angle θ with the CuO_2 planes. The solid line is the best fit to $\Delta H(\theta)=\Delta H(0)/\cos\theta$.

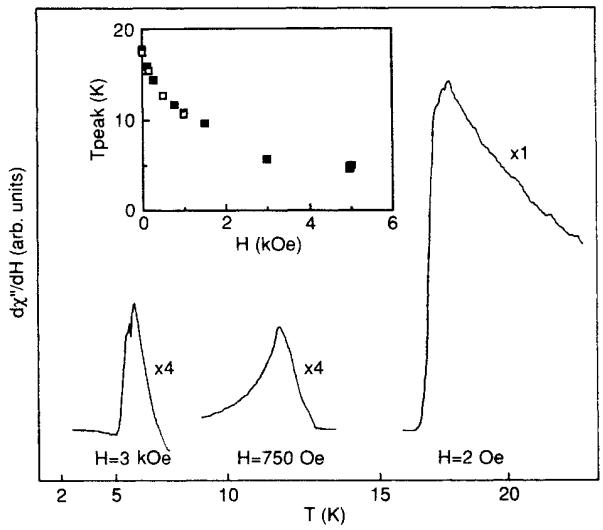

FIG. 16. Microwave magnetoabsorption as a function of temperature for Gd_2CuO_4 in different magnetic fields applied parallel to the CuO_2 planes at 9 GHz. Inset: Position of the *S*-6 signal peak as a function of field component along the CuO_2 planes for the same sample. The solid squares (■) correspond to data taken for various fields applied parallel to the CuO_2 planes. The open squares (□) correspond to data taken with a field of 5 kOe making an angle θ with the planes where the temperature of the peak is then plotted as a function of the component of field in the plane, 5 kOe $\cos\theta$.

D. Electron paramagnetic resonance (EPR)

We do not observe any EPR signal that we can identify with Cu^{2+} in any of the systems studied over the temperature range 2–600 K. Possible reasons for the absence of the Cu^{2+} signal will be addressed in the analysis.

The only EPR signal we have observed and identified in these systems is that due to Gd^{3+}. We have previously reported our measurements for the system $Eu_{2-x}Gd_xCuO_4$, where we found that for $x=0.03$ the spectra correspond to the fine structure expected for a Gd^{3+} free ion in a tetragonal host.[18] For $x>0.2$ we found a single, broad Gd^{3+} EPR line.[13]

For $PrGdCuO_4$ and $NdGdCuO_4$, which do not exhibit the signatures *S*-1 through *S*-6, we also find a single Gd^{3+} EPR line with a field for resonance, H_r, corresponding to $g\sim2.00$ over the full temperature range, 2–300 K. There is a small angular dependence of H_r that is consistent with sample demagnetization effects.

The behavior of H_r for $PrGdCuO_4$ and $NdGdCuO_4$ just summarized is in marked contrast to that which we observe for Gd-doped samples that do exhibit the *S*-1 to *S*-6 signatures. For these samples, the Gd^{3+} EPR signal above 270 K behaves exactly as that of the nonsignature samples just discussed.[19] However, for temperatures below 270 K the field for resonance, H_r, develops an anomalous angular dependence, which we call the signature *S*-7. As an illustration of the large shifts of H_r that are observed, we present the 35 GHz spectra shown in Fig. 17. Note that the center of the Gd^{3+} resonance signal is $\sim$2 kOe above that for the diphenylpicrylhydrazyl (DPPH) marker at $g\approx2.00$. (The midfield absorption shown in Fig. 17 is also strongly shifted to higher fields when compared to that in Fig. 10, because of the choice of field angle, temperature, and the use of a higher spectrometer frequency.)

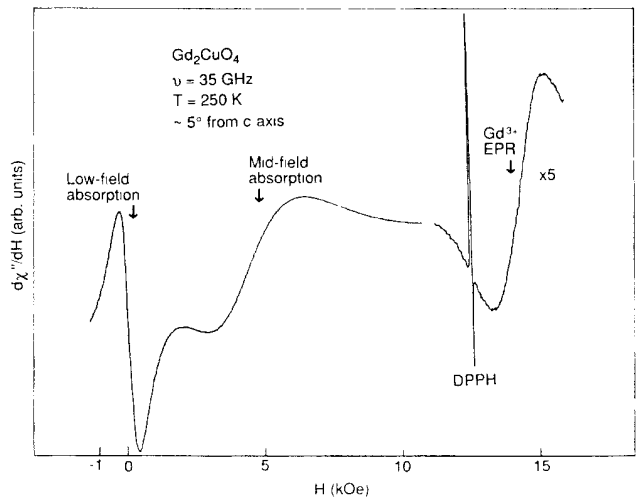

FIG. 17. Spectrum for a 0.3 mg single crystal of Gd_2CuO_4 measured at 250 K and 35 GHz with the field applied $\sim5°$ from the *c* axis, so the low-field absorption, midfield absorption, and Gd^{3+} EPR signals are all resolved. The DPPH is used as a marker. Notice the substantial shift from $g=2.00$ for the Gd^{3+} EPR line.

1. S-7: anomalous anisotropy in the Gd^{3+} EPR field for resonance

We have made an extensive study of the temperature, frequency, and field angle dependence of the EPR signal for the sample series $Eu_{2-x}Gd_xCuO_4$ $(0.2\le x\le2)$, $Tb_{2-x}Gd_xCuO_4$ $(1\le x\le2)$, and $SmGdCuO_4$. As an example of the nature of the *S*-7 signature, in Fig. 18 we present the shift of H_r from H_0 (the field corresponding to $g=2.00$) for a Gd_2CuO_4 sample as a function of the angle θ, for two temperatures and two microwave frequencies. First, we note that the behavior is independent of frequency, indicating the shift is due to the presence of an internal effective field (i.e., not a true *g* shift). Second, as previously stated, above 270 K, H_r is nearly independent of θ, whereas below 270 K we find that H_r exhibits extreme out-of-plane anisotropy (it remains isotropic in the *a*-*b* plane). In the inset of Fig. 18 we present the temperature dependence of H_r for two field angles. From these data one can readily identify T_h at which the out-of-plane anisotropy sets in, and T_L, at which the anisotropy un-

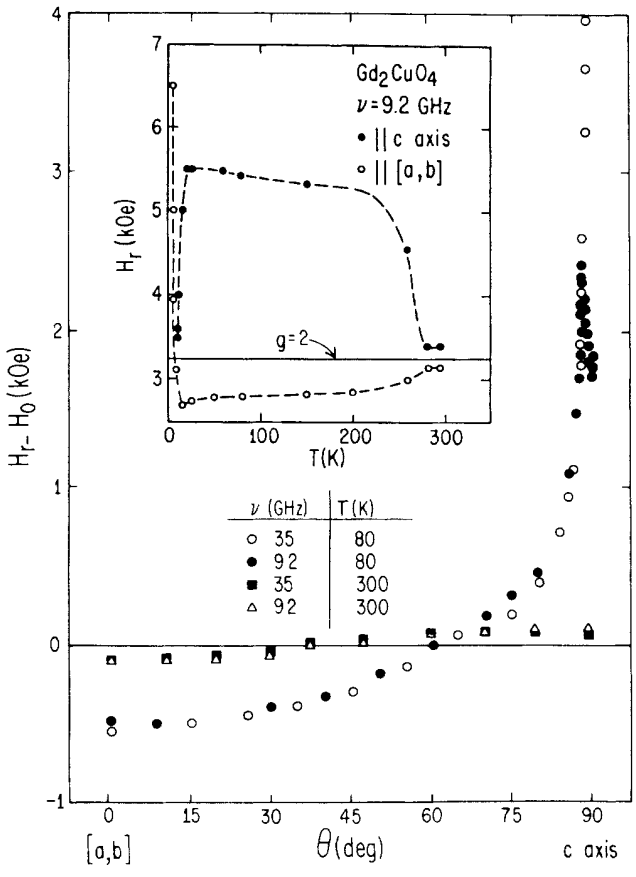

FIG. 18. The field shift of the EPR of the Gd^{3+} ion in Gd_2CuO_4, relative to that for $g=2$, vs θ, the angle of the applied field relative to the *a*-*b* plane for the temperatures and frequencies indicated. Above 270 K, H_r is basically independent of angle, whereas below and down to $\sim$19 K, there is the anisotropic behavior shown. Inset. H_r vs temperature for $\theta=0°$ and 90°. Note the rapid changes in H_r at temperatures near T_h and T_L.

dergoes a rapid change of character.

We find the same shift for all three systems studied ($R_{2-x}Gd_xCuO_4$ with R=Eu, Tb, or Sm). The magnitude of the shift in H_r (once fully developed) at $\theta=0$ is $H_r-H_0=500\pm150$ Oe, a value somewhat smaller than the 800 ± 200 Oe deduced for $H_i(0)$ from the weak ferromagnetism (*S*-3). If the $H_i(\theta)$ deduced from the weak ferromagnetism were the only source that contributed to the shift, one would expect H_r-H_0 to go to zero at $\theta=90°$. Instead, as is seen in Fig. 18, it goes through zero at $\theta\sim60°$, and then continues to extreme positive values as θ approaches 90°. Notice that within a few degrees of the *c* axis, H_r for 9.2 GHz data drops sharply, although this feature is not observed in the 35 GHz data. Further evidence for an anomalous behavior close to the *c* axis is presented in Fig. 19 for $EuGdCuO_4$, where we present the H_r, peak-to-peak linewidth (ΔH_{pp}), and signal peak-to-peak amplitude (A_{pp}), as a function of field angle. All show a dramatic drop very close to the *c* axis. We tentatively interpret these data as indicative that the component of the magnetic field parallel to the planes has dropped below that value needed to "saturate" the weak ferromagnetism as illustrated in Fig. 4 and discussed under *S*-3.

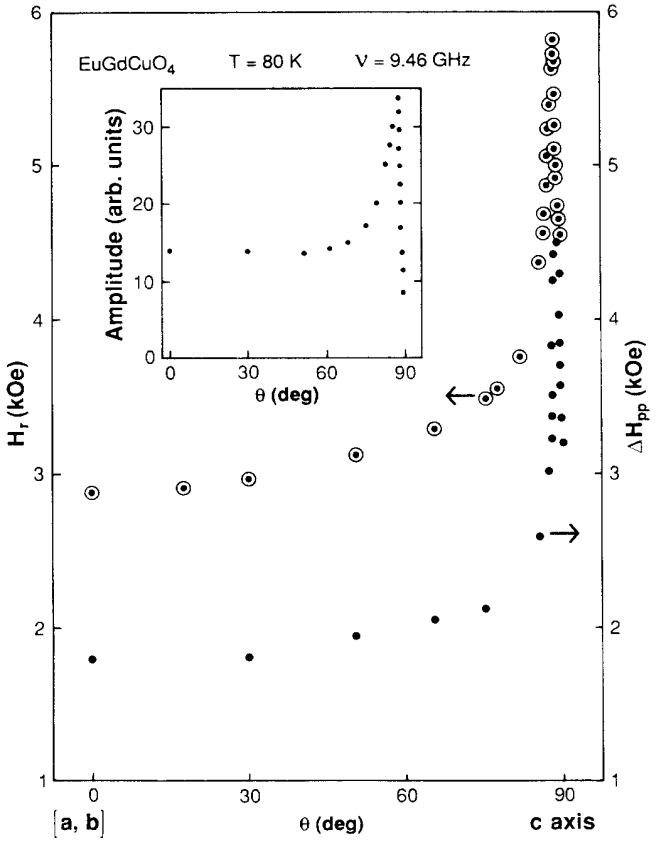

FIG. 19. Resonance field (H_r) and linewidth (ΔH_{pp}) for the Gd^{3+} EPR signal of a single crystal of $EuGdCuO_4$ measured at 80 K and 9.46 GHz with the field making an angle θ with the CuO_2 planes. Notice the sharp drop in H_r and ΔH_{pp} when θ approaches 90°. Inset: The amplitude of the EPR line as a function of angle. The large increase of the amplitude occurs at the same time that the ΔH_{pp} increases, contrary to what is typically expected.

E. *S*-8: specific heat

For Nd, Sm, and Gd, there is a peak in the specific heat, C_p (signature *S*-8) that is taken to be a consequence of the antiferromagnetic ordering of their moments.[20] In Table I we present the temperatures at which the peak occurs. No ordering has been observed for Pr and Eu down to 1.5 K. The specific-heat measurements of $Eu_{2-x}Tb_xCuO_4$ between 1.5 and 25 K for $x=0.5$ and 1 show an interesting behavior. In Fig. 20 we present the C_p as a function of temperature for $EuTbCuO_4$. The broad maximum at ~3 K as shown for $x=1$ shifts to 1.5 K when $x=0.5$, suggesting a progressive spin freezing out of local disorder.[21]

IV. ANALYSIS AND DISCUSSION

A. Why some samples show signatures and others do not

If all the R_2CuO_4 do order similarly at ~270 K, the question is raised as to why some compounds show the signatures *S*-1 to *S*-7, and others do not. A possible explanation may be related to the small differences in the *R* ionic radii. In Fig. 21 we plot the lattice parameter, *a*, versus the rare-earth atomic number for compositions as indicated in the figure. The compounds studied may be divided into two groups; those that show signatures *S*-1 to *S*-7, and those that do not, as indicated by the dashed curve. The first group always contains the smaller-sized rare-earth atoms: $R\equiv$Gd, Tb, or Dy. The second group contains the largest: $R\equiv$Pr, Nd, Sm, or Eu. As progressively smaller *R* atoms are substitutied into the R_2CuO_4, a crystallographic distortion may become favorable. This may explain why the signatures *S*-1 and *S*-7 are found in Gd_2CuO_4 and not in Eu_2CuO_4 or Nd_2CuO_4. For example, when Eu and Nd are partially replaced by Tb and Dy, respectively, to form $EuTbCuO_4$ and $NdDyCuO_4$,

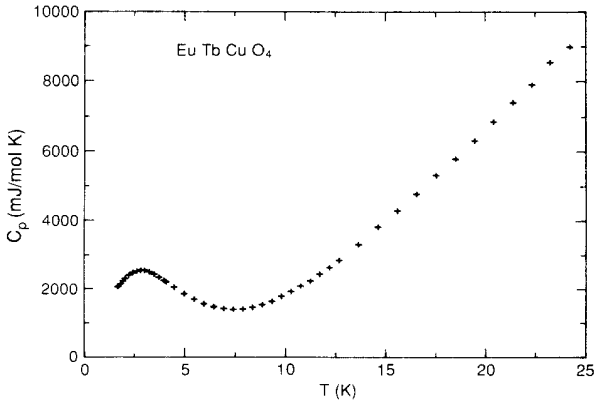

FIG. 20. Specific heat, C_p, as a function of temperature for $EuTbCuO_4$. The broad maximum at ~3 K shifts to lower temperature and becomes weaker when the concentration of Tb is reduced.

the average ionic radii are then closer to that of Gd^{3+}, and the conditions for observing the signatures *S*-1 to *S*-7 may again become favorable.

B. Intepretation of T_h

Recent muon spin rotation and neutron scattering studies in Pr_2CuO_4, Nd_2CuO_4, and Sm_2CuO_4 have suggested that the copper moments order antiferromagnetically in the plane with a Néel temperature, T_N, between 255–270 K.[22–25] We do not observe the *S*-1 to *S*-7 signatures in these pure compounds (which coincidentally are the ones which so far have been shown to become superconductors when doped with Ce or Th),[7–10] although we do see them in the mixed $NdDyCuO_4$ and $SmGdCuO_4$ versions. From the neutron scattering experiments, and in analogy to the La_2CuO_4 insulating compound,[3] we identify T_h, as discussed in Sec. III, with a three-dimensional (3D) Néel transition, T_N. Even though we do not observe the signature anomalies identifying T_h in all the R_2CuO_4 compounds shown in Table I, we expect that all versions undergo a 3D antiferromagnetic transition with their T_N close to 270 K. The *S*-1, *S*-3, *S*-4, *S*-5, and *S*-7 signatures are typically fully established a few degrees below ~270 K, and their properties are basically independent of temperature down to T_L. A common feature found in signatures *S*-1 to *S*-7 is a large out-of-plane anisotropy (not found in any signal above T_h), which further supports the basic 2D nature of the CuO_2 planes.

As noted, all combinations of rare earths studied gave almost the same value of T_h (when observed). However, we found that when Gd is replaced by Ce or Th, or Cu is replaced by Ni, T_h is depressed.

C. The meaning of T_L

In contrast to T_h, the value of T_L depends on the rare earths used. At T_L dramatic changes occur in most signatures. For example, the large changes in the H_r of Gd^{3+} (signature *S*-7) shown in the inset of Fig. 18 correlate with the rapid changes observed in the dc and ac magnetization at T_L. A plausible explanation for the behavior seen at T_L is that the exchange interaction between the Cu and *R* ions is sufficient to cause the Cu to undergo a spontaneous spin reorientation, similar to that observed in the orthoferrites.[26]

D. The consequences of a distortion from tetragonal symmetry

A possible interpretation of the *S*-3 signature, i.e., the weak ferromagnetism that depends only on the component of the magnetic field in the plane, is that there is a canting of the copper moments away from strictly antiferromagnetic alignment. A similar interpretation was invoked in the orthoferrites by Cooke *et al.*[26] The origin of the spin canting is attributed to an antisymmetric exchange interaction, as discussed by Dzyaloshinsky[27] and Moriya.[28] Implicit in this interpretation is the assumption that the Cu-O coordination is no longer square planar, since in crystals with true tetragonal symmetry, the antisymmetric coupling cancels, and the Dzyaloshinsky-Moriya interaction is no longer effective.[28] If the canted component were ordered it would produce an internal field at the *R* site in the direction of the *a*-*b* plane. Following Cooke *et al.*,[26] we can estimate the canted copper moment, M_{Cu} by writing the measured magnetization as

$$M = M_{Cu} + C_R(H_i + H_a)/(T + \Theta_R) , \quad (1)$$

where C_R is the Curie constant for the rare-earth, Θ_R is the Curie-Weiss temperature, and H_a the applied field. The common intersection point for the curves in Fig. 5 gives $M_{Cu} \leq 10 \pm 10$ emu/mol, which is equivalent to $\sim 2 \pm 2 \times 10^{-3} \mu_B$/Cu. Unfortunately, there is a large uncertainty in this result, but the sign of the M_{Cu} is such that the ferromagnetic component of Cu is in the direction of the applied field. The average value of M_{Cu} is similar to the weak ferromagnetic moment, $\sim 3 \times 10^{-3} \mu_B$/Cu reported in La_2CuO_4.[29]

Within the experimental error, we never detect a magnetic remanence. Instead, there is a sharp increase of the initial magnetization with applied magnetic field, as seen in Figs. 3–5. It seems that a small, but finite, magnetic field is necessary to "turn on" the mechanism that leads to the observed anisotropic properties. One possibility is that there are basically antiferromagnetic domains, but with slightly canted Cu moments that can be aligned by a small magnetic field. Such a picture could also explain the strong dependence on applied magnetic field of *S*-1 or *S*-5. The broad shoulder, found above *S*-1 in the ac susceptibility (Fig. 9), may also be indicative of short-range order. A similar dependence on the magnetization was recently reported for α-$TlMnCl_3$.[30]

In the description of the *S*-3 data in Sec. III A we mention that in Gd_2CuO_4 the magnetization is nearly independent of field orientation in the plane, while for $EuTbCuO_4$ there is a large anisotropy. One possible explanation is that for $EuTbCuO_4$ there is additional symmetry breaking induced by magnetoelastic stress placed on the lattice by the copper ordering process.[31] Such a small distortion could be consistent with the absence of any observed difference in the ratio of lattice parameters (a,b) at temperatures well below T_N, as measured by x rays.

E. Angular anisotropy

Independent of the mechanism responsible for H_i, data similar to that illustrated in Figs. 4 and 5 may be analyzed at all temperatures between T_h and T_L to yield an H_i with a value of ~800 Oe, nearly independent of *R*. A feature common to several signatures is that they only depend on the component of field in the *a*-*b* plane. This is illustrated by the data shown in Figs. 13–15, 18, and 19. These data exhibit a $K/\cos\theta$ dependence that may be interpreted as requiring an applied field at any angle θ, of such a magnitude that the component of field in the plane has the constant value *K*.

Additional examples of anisotropy are the field required to reach the linear portion of the *M* versus *H*

curve for the signature S-3 as shown in Fig. 7, or the field required to produce a peak at a given temperature in the magnetoabsorption signal S-6 as shown in Fig. 16.

F. EPR of Gd^{3+}

The only EPR signal observed and identified is for Gd^{3+}, which has an $^8S_{7/2}$ ground state. For systems where the S-1 through S-6 signatures are not present, as in Pr (or Nd) $GdCuO_4$, the Gd^{3+} resonance field, H_r, and the linewidth, ΔH_{pp}, are essentially independent of angle at any temperature. Apparently, the Gd^{3+} resonance does not reflect the antiferromagnetic ordering at ~ 270 K found by the neutron and muon studies.[22–25] In contrast, in the group of compounds where the other signatures are present, the H_r for Gd^{3+} has an unexpected angular dependence below T_h. At temperatures above T_h, H_r, as corrected for sample demagnetization, is essentially independent of θ, as illustrated for $T=300$ K in Fig. 18. As further illustrated in Figs. 18 and 19, at all temperatures between T_h and T_L the shift in H_r from H_0 is very anisotropic. Since the magnitude of this shift is basically independent of frequency, it reflects an internal field, and not a change in g value. The amount the shift in H_r is about 500 Oe at $\theta=0$, which is in the correct direction, but is significantly smaller than the ~ 800 Oe deduced for $H_i(0)$ from the M_{dc} data. As previously mentioned, if the only mechanism which contributes to the shift were the one associated with H_i, one would expect H_r-H_0 to go to zero at $\theta=90°$. Instead, as is seen in Figs. 18 and 19, it goes through zero at $\theta\sim 60°$, and then continues to extreme positive values as θ approaches 90°. We try to represent the angular dependence of H_r with the following expression:

$$H_r(\theta)=H_0-H_i(0)\cos\theta+K'/\cos\theta\ , \tag{2}$$

where $H_i(0)$ is taken to be 800 Oe, and K' is chosen for the best fit to the data. Equation (2), with $K'\approx 300$ Oe represents the data fairly well until a few degrees from the c axis, at which point H_r (for the 9.2 GHz) data drops sharply, a feature not contained in Eq. (2). We attribute the sharp drop to be a consequence of there no longer being a large enough component of the applied field in the a-b plane to fully "set" the weak ferromagnetism as required from the data in Fig. 4. We infer that this feature is not observed in the 35 GHz data because we cannot align the crystal accurately enough to the c axis to achieve a small enough projected component of the field in the plane, as the magnitude of the applied field necessary to observe the Gd^{3+} resonance is ~ 3.5 times larger than at 9.2 GHz.

As seen in Fig. 19 for $EuGdCuO_4$, the linewidth and the amplitude have the same angular dependence as H_r. Such a behavior might be expected for the linewidth because, due to the large shifts in H_r, any sample inhomogeneity would be reflected as a superposition of a spread in lines. However, the amplitude would then be expected to decrease as the linewidth increases, contrary to what is observed. We note that H_r, ΔH_{pp}, and the amplitude, all decrease rapidly within a few degrees of the c axis, presumably reflecting the incomplete "setting" of the field in the plane noted earlier.

G. Midfield absorption

The midfield absorption, S-4, is the most pervasive of all the signatures listed in Table I. If any of the other signatures are present, it is always observed and it is the only signature found in pure Eu_2CuO_4. Note that in Fig. 21 the lattice parameter for Eu_2CuO_4 is close enough to the dashed boundary that one might expect signatures to be present in this compound. The addition of only 1 at. % of Gd is sufficient for other signatures, e.g., S-1, to appear.[17] The intensity of the midfield absorption corresponds to a large effective moment per formula unit, between 3 and $100\mu_B$. The larger values imply a cooperative response within the spin system. This suggests that we may be observing the resonance of spin clusters or domains that in turn feel an internal field due to the anisotropic exchange interactions. The anomalous dependence of the midfield absorption signal on the frequency of the modulating field could also be indicative of a domain structure, where some internal domain relaxation time is comparable to the modulation frequency. The midfield absorption signal always appears a few Kelvins above the onset of the S-5 signature, which again may be indicative of short-range ordering prior to the true 3D transition.

Both H_p and the associated linewidth follow the relation $H(\theta)=H(0)/\cos\theta$, as seen in Figs. 13, 14, and 15 (inset). Similar angular dependence of the resonance field

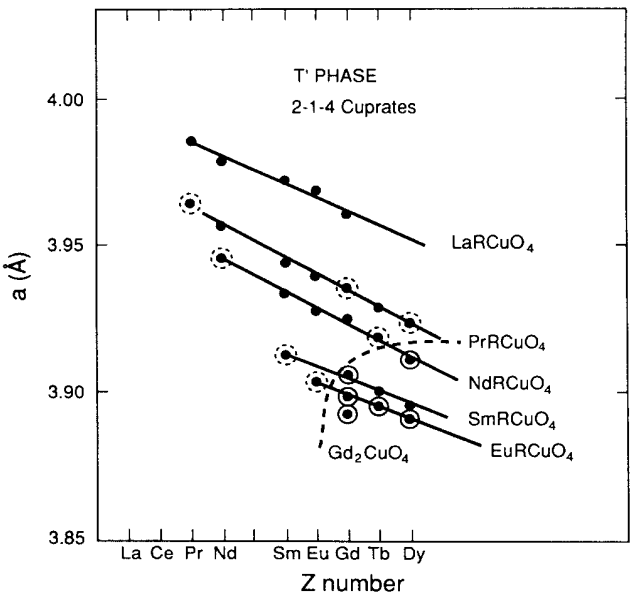

FIG. 21. Lattice parameter, a, as a function of rare-earth atomic number for the host compounds indicated. The solid points are data obtained from the literature. Circled points indicate the compounds we have studied. The dashed curve shows the boundary between samples that exhibit the signatures S-1 to S-7 (solid-circled points) and those which do not (dashed-circled points).

and linewidth, and temperature dependence of the amplitude (shown in Fig. 15) have been found in other 1D and 2D systems where the EPR line is associated with spin-cluster resonances.[32,33]

The field for resonance of the midfield absorption is a function of frequency, which is further evidence for it being some form of spin resonance. However, we note that the signal does not go to zero when the rf magnetic field is parallel to the dc field.

H. Low-field absorption

The low-field absorption, *S*-5, is the most difficult signature to fully characterize because it appears at very low fields (where it is may overlap *S*-4), and because it appears to evolve in a complex way with temperature near T_L and T_h. However, at temperatures where it is well resolved, the field at which the signal peaks depends on the angle, θ, of the dc field to the a-b plane as $1/\cos\theta$.

I. Ordering of the *R* moments

Both the specific-heat and magnetic-susceptibility measurements of R_2CuO_4 indicate antiferromagnetic order at about 1.5, 6, and 6.5 K, for R=Nd, Sm, and Gd, respectively.[20] We cannot associate T_L with the incipient antiferromagnetic ordering of the R moments, because Nd_2CuO_4 and Sm_2CuO_4, which do not show any of the signatures, both order, whereas $EuTbCuO_4$, which exhibits all of the signatures, does not. Notice that the specific heat of $EuTbCuO_4$ shown in Fig. 20 has a broad Schottky type of maximum that strongly depends on the concentration of Tb. This behavior can be interpreted as a progressive freezing of the spins out of local disorder, where there is a spread of magnetic exchange constants, including those beyond nearest-neighbor interactions between the Tb ions.[21,34]

J. The Cu^{2+} moment problem

1. The dc magnetization

For layered magnetic systems one expects significant deviations from free-ion magnetic behavior for temperatures less than $\sim 3T_N$.[21] We can seek to determine the contribution of the Cu^{2+} ions to M_{dc} in this temperature range, but unfortunately the large M_{dc} of the R ions makes this quite difficult. If, at the highest temperature measured, $\sim$700 K, the Cu^{2+} contributed with a full $S=\frac{1}{2}$ moment, they would consitute $\sim$5% of the total M_{dc} for the Gd and 25% for the Pr or Nd compounds. As can be seen, the inverse susceptibility data for Pr_2CuO_4 and Nd_2CuO_4 presented in Fig. 1 are linear, and between 100 and 700 K can be well fit with $\mu_{eff}=3.66\pm0.05\mu_B$, $\Theta_R\sim-65$ K for Pr, and $\mu_{eff}=3.56\pm0.05\mu_B$, $\Theta_R\sim-60$ K for Nd. From these data we conclude that the contribution of Cu^{2+} in the Pr or Nd compounds is $\leq 0.4\pm0.2\mu_B$/Cu. The small moment of Sm^{3+} in Sm_2CuO_4, $\sim 0.5\mu_B$/ion, suggests that it might be the optimum system to determine the contribution of Cu^{2+} to the magnetization. However, a similar analysis for Sm_2CuO_4 is complicated because Sm^{3+} has a $J=\frac{5}{2}$ level as a ground state, split into three doublets by the tetragonal crystal field. As a result of the large admixture with low-lying J multiplets (as also frequently seen in other Sm compounds),[35] it is necessary to take into account the populations of levels other than the ground state. These levels are all split by crystal-field effects, and one must also include second order Zeeman terms. As a consequence of these effects it is more difficult to determine the effective Cu^{2+} moment from the Sm compound magnetization data than would at first appear.

2. The effect of a Cu^{2+} dipolar field on the Gd EPR

The EPR data for dilute Gd in $Eu_{2-x}Gd_xCuO_4$ ($x=0.03$) may be interpreted to set a limit on the magnitude of the ordered Cu moment by the following analysis. If the Cu moments are ordered antiferromagnetically in the plane, and have a full moment expected for $S=\frac{1}{2}$, there will be a net static dipolar magnetic field at alternating R sites of $\sim\pm800$ Oe. (Since the field alternates direction at the R sites, it cannot be responsible for the H_i of *S*-3). If the dipolar field was parallel to the applied field it would result in a splitting of the Gd^{3+} EPR signal of about 1600 Oe. From the observed spectra we conclude that if the fields are parallel, then the effective magnetic moment is ≤ 0.3 of that expected for a spin $\frac{1}{2}$. If the fields were perpendicular, however, there would primarily be a small reduction in H_r ($\sim$100 Oe) with a greatly reduced splitting due only to any angular anisotropy of the resonance, in which case our data would not set a meaningful limit.

3. Why is the EPR of the Cu^{2+} ion not observed?

The nature of EPR in 2D antiferromagnetic compounds has been studied in several systems, and in most cases an EPR signal is observed only well above T_N.[21,36–38] At temperatures of $\sim 3T_N$ the linewidth decreases slowly as the temperature is reduced, passing through a minimum at $\sim 2T_N$, and subsequently increases anomalously when approaching T_N from above. Since we believe that the 3D ordering temperature is of the order of T_h for the R_2CuO_4 system, the fact that we do not observe any Cu EPR signal at temperatures up to 600 K in these compounds suggests that the 2D antiferromagnetic correlations are strong even for $T\geq 2T_N$, or there are other mechanisms operative that broaden the Cu EPR signal beyond detectable limits.

We note that the typical observation of the narrowest EPR signal at $\sim 2T_N$ for many 2D antiferromagnetic systems clearly does not seem to be obeyed in the other copper-oxide superconducting systems. (The absence of a Cu^{2+} EPR signal has been reported previously by us and other authors for the other copper-oxide superconductors and their parent compounds, La_2CuO_4 and $RBa_2Cu_3O_6$.[39,40]) That is, when the La or 1:2:3 versions are doped to suppress the Néel temperatures, one still does not observe a Cu^{2+} EPR signal at any temperature, including those in the vicinity of $2T_N$. Thus, this "rule of

thumb" based on other systems is not appropriate. One explanation may be that the intraplanar exchange is really much larger than that inferred from the observed T_N, and that other conditions, such as hole doping, reduce the observed 3D ordering temperature, but not the underlying 2D spin correlations in an equivalent manner.

V. CONCLUSIONS

From our data and recent neutron-diffraction[22–24] and muon precession measurements,[25] we conclude that all the R_2CuO_4 compounds studied here order antiferromagnetically in a quasi-two-dimensional arrangement at ~ 270 K with the Cu moments strongly coupled within the CuO_2 layers. The presence of long-range 2D antiferromagnetic spin correlations, well above T_N, is supported by the negligible contribution of the Cu moments to the dc magnetization, $\leq 0.4\mu_B$/Cu, and the total absence of a Cu^{2+} EPR signal up to 600 K. This behavior is similar to that reported for La_2CuO_4, which is also a 2D antiferromagnetic insulator below 300 K.

Below $T_h \sim 270$ K, the compounds can be divided into two groups, one where the signatures S-1 to S-7 as described are present, and the other where they are not. The presence of these signatures may be due to a distortion of the tetragonal arrangement of the Cu ions, which in turn produces an internal field at the R sites. Such a distortion may also induce the formation of spin-canted antiferromagnetic domains that may be aligned by a small external field. This picture could explain the presence of the weak ferromagnetism (S-3), the midfield absorption (S-4), and the magnetic field dependence of the S-1 peak.

A common feature of the diverse signatures is their unusual dependence on the angle and magnitude of the applied magnetic field. It appears that, for those samples that exhibit the S-1 to S-7 signatures, there is a minimum component of field needed in the a-b plane to fully establish their character. Equation (2) at least provides an empirical description for the angular dependence of the Gd^{3+} EPR signal, however, the physical origin of the several terms describing the shift in H_r is not known.

T_L is tentatively attributed to a spontaneous spin reorientation of the canted Cu ions. In contrast to T_h, T_L depends on the R used, but it does not appear to be directly associated with any antiferromagnetic ordering that may occur at lower temperatures.

We suggest that further investigation of the complex magnetic properties of the R_2CuO_4 compounds and their doped superconducting versions is warranted, and that once clarified, the signatures described herein will be useful monitors to further our understanding of the role of magnetism in the high-temperature superconducting copper oxides.

ACKNOWLEDGMENTS

We wish to thank R. Goldfarb and R. L. Spomer for measuring the ac susceptibility data presented. We thank H. Shore, D. Fredkin, and R. Goldfarb for helpful conversations, and R. Isaacson for his technical assistance. This research was partially supported at San Diego State University by the National Science Foundation (NSF) under Grant Nos. NSF-DMR-88-01317 and NSF-INT-89-00851, at the University of California–San Diego by Grant Nos. NSF-DMR-86-13858 and ONR-NOOO14-87-K-0338, and the work at Los Alamos National Laboratory was performed under the auspices of the United States Department of Energy.

[1]See, for example, G. Aeppli, in *1st Topsoe Summer School in Superconductivity*, edited by N. H. Anderson and K. Mortenson (Riso, National Laboratory, Roskilde, Denmark, 1988), p. 47; and S-W. Cheong, J. D. Thompson, and Z. Fisk, Physica **158C**, 109 (1989).

[2]See, for example, W. E. Pickett, Rev. Mod. Phys. **61**, 433 (1989).

[3]J. M. Tranquada, D. E. Cox, W. Kunnmann, J. Moudden, G. Shirane, M. Suenaga, P. Zolliker, D. Vaknin, S. K. Sinha, M. S. Alverez, A. J. Jacobsen, and D. C. Johnston, Phys. Rev. Lett. **60**, 156 (1988); J. W. Lynn, W.-H. Li, J. A. Mook, B. C. Sales, and Z. Fisk, *ibid.* **60**, 2781 (1988); D. C. Johnson, J. P. Stokes, D. P. Goshorn, and J. T. Lewandowski, Phys. Rev. B **36**, 4007 (1987).

[4]R. J. Birgeneau and G. Shirane, *Physical Properties of High Temperature Superconductors*, edited by D. M. Ginsberg (World Scientific, Singapore, in press).

[5]D. C. Johnston, J. P. Stokes, D. P. Goshorn, and J. T. Lewandowski, Phys. Rev. B **36**, 4007 (1987); D. C. Johnston, S. K. Sinha, A. J. Jacobson, and J. M. Newsam, Physica **153-155B**, 572 (1988); D. C. Johnson, W. C. Lee, D. P. Goshorn, J. T. Lewandowski, Y. Hidaka, T. Murakami, and C. F. Keweshan (unpublished).

[6]J. E. Schirber, B. Morosin, R. M. Merrill, P. R. Heave, E. L. Venturini, J. F. Kwak, P. J. Nigrey, R. J. Baughman, and D. S. Ginly, Physica **152C**, 121 (1988).

[7]Y. Tokura, H. Takagi, and S. Uchida, Nature (London) **337**, 345 (1989).

[8]H. Takagi, S. Uchida, and Y. Tokura, Phys. Rev. Lett. **62**, 1197 (1989).

[9]J. T. Markert and M. B. Maple, Solid State Commun. **70**, 145 (1989).

[10]J. T. Markert, E. A. Early, T. Bjornholm, S. Ghamaty, B. W. Lee, J. J. Neumier, R. D. Price, C. L. Seaman, and M. B. Maple, Physica **158C**, 178 (1989).

[11]J. M. Tranquada, S. M. Heald, A. R. Moodenbaugh, G. Liang, and M. Croft, Nature (London) **337**, 720 (1989).

[12]Hk. Muller-Buschbaum and W. Wollschlager, Z. Anorg. Allg. Chem. **414**, 76 (1975); B. Grande, Hk. Muller-Buschbaum, and M. Suhweizer, *ibid.* **428**, 120 (1977).

[13]S. B. Oseroff, D. Rao, F. Wright, M. Tovar, D. C. Vier, S. Schultz, J. D. Thompson, Z. Fisk, and S-W. Cheong, Solid State Commun., **70**, 1159 (1989).

[14]K. A. Kubat-Martin, Z. Fisk, and R. R. Ryan, Acta Crystallogr. Sect. C **44**, 1518 (1988).

[15]G. R. Stewart, Rev. Sci. Intrum. **54**, 1 (1983).

[16]R. B. Goldfarb and J. V. Minervini, Rev. Sci. Instrum. **55**, 761 (1984); R. B. Goldfarb, Ph.D. thesis, Colorado State Universi-

ty, 1979 (unpublished).
[17]J. D. Thompson, S-W. Cheong, S. E. Brown, Z. Fisk, S. B. Oseroff, M. Tovar, D. C. Vier, and S. Schultz Phys. Rev. B **39**, 6660 (1989).
[18]D. Rao, M. Tovar, S. B. Oseroff, D. C. Vier, S. Schultz, J. D. Thompson, S-W. Cheong, and Z. Fisk, Phys. Rev. B **38**, 8920 (1988).
[19]For some Gd-doped samples with $x < 0.05$ we do not observe the Gd^{3+} EPR signal, which we tentatively attribute to an enhanced relaxation rate due to coupling with the dominant R ion.
[20]M. F. Hundley, J. D. Thompson, S-W. Cheong, Z. Fisk, and S. B. Oseroff, Physica **158C**, 102 (1989).
[21]L. J. de Jongh and A. R. Miedena, Adv. Phys. **23**, 1 (1974).
[22]D. C. Cox, A. I. Goldman, M. A. Subramanian, J. Gopalakrishnan, and A. W. Sleight, Phys. Rev. B **40**, 6998 (1989).
[23]S. Skanthakumar, Z. Zhang, T. W. Clinton, W. H. Li, J. W. Lynn, Z. Fisk, and S-W. Cheong, Physica **160C**, 124 (1989).
[24]Y. Endoh, M. Matsuda, K. Yamado, K. Kakurai, Y. Hidaka, G. Shirane, and R. J. Birgeneau, Phys. Rev. B **40**, 7023 (1989).
[25]G. M. Luke, B. J. Sternlieb, Y. J. Uemura, J. H. Brewer, R. Kadono, R. F. Kiefl, S. R. Kretizman, T. M. Riseman, J. Gopalakrishnan, A. W. Sleight, M. A. Subramanian, S. Uchida, H. Takagiana, and Y. Tokura, Nature (London) **338**, 49 (1989).
[26]A. H. Cooke, D. M. Martin, and M. R. Wells, J. Phys. **7C**, 3133 (1974).
[27]I. Dzyaloshinsky, J. Phys. Chem. Phys. Solids **4**, 241 (1958).
[28]T. Moriya, Phys. Rev. **120**, 91 (1960).
[29]S.-W. Cheong, Z. Fisk, J. O. Willis, S. E. Brown, J. D. Thompson, J. P. Remeika, A. S. Cooper, R. M. Aikin, D. Schieferl, and G. Gruner, Solid State Commun. **65**, 111 (1988); S-W. Cheong, J. D. Thomspon, Z. Fisk, and G. Gruner, *ibid.* **66**, 1019 (1988).
[30]T. A. Velikanova, A. D. Balaev, and N. V. Fedoseeva, Fiz. Tverd. Tela (Leningrad) **29**, 283 (1987) [Sov. Phys.—Solid State **29**, 164 (1987)].
[31]See, for example, A. H. Morrish, *The Physical Properties of Magnetism* (Wiley, New York, 1965), p. 321.
[32]K. Adachi, Phys. Soc. Jpn. **50**, 3904 (1981).
[33]Y. Ajiro, K. Adachi, and M. Mekata, J. Magn. Magn. Mater. **31-34**, 1141 (1983).
[34]M. T. Causa, S. M. Dutrus, C. Fainstein, R. Sanchez, L. B. Steren, M. Tovar, R. Zysler, S. B. Oseroff, D. C. Vier, S. Schultz, Z. Fisk, and J. L. Smith, Physica **153-155C**, 188 (1988).
[35]H. W. de Wijn, A. M. van Diepen, and K. H. J. Buschow, Phys. Status Solidi B **76**, 11 (1976).
[36]L. J. de Jongh, Solid State Commun. **65**, 963 (1988).
[37]P. M. Richards and M. B. Salamon, Phys. Rev. B **9**, 32 (1974).
[38]H. van der Vlist, A. F. M. Arts, and H. W. de Nijn, Phys. Rev. B **30**, 5000 (1984).
[39]D. C. Vier, S. B. Oseroff, C. Salling, J. F. Smyth, S. Schultz, Y. Dalichaouch, B. W. Lee, M. B. Maple, Z. Fisk, and J. D. Thompson, Phys. Rev. B **36**, 8888 (1987).
[40]F. Mehran, S. E. Barnes, G. V. Chandrashekhar, T. R. McGuire, and M. W. Shafer, Solid State Commun. **67**, 1187 (1988).